

# Left-right asymmetry for pion and kaon production in the semi-inclusive deep inelastic scattering process

Bo Sun, Jun She, Bing Zhang, Ya-Jun Mao, and Bo-Qiang Ma

School of Physics and State Key Laboratory of Nuclear Physics and Technology, Peking University, Beijing 100871, China,  
e-mail: maoyj@pku.edu.cn  
e-mail: mabq@phy.pku.edu.cn

Received: date / Revised version: date

**Abstract.** We analyze the left-right asymmetry in the semi-inclusive deep inelastic scattering (SIDIS) process without introducing any weighting functions. With the current theoretical understanding, we find that the Sivers effect plays a key role in our analysis. We use the latest parametrization of the Sivers and fragmentation functions to reanalyze the  $\pi^\pm$  production process and find that the results are sensitive to the parametrization. We also extend our calculation on the  $K^\pm$  production, which can help us know more about the Sivers distribution of the sea quarks and the unfavored fragmentation processes. HERMES kinematics with a proton target, COMPASS kinematics with a proton, deuteron, and neutron target (the information on the neutron target can be effectively extracted from the  $^3\text{He}$  target), and JLab kinematics (both 6 GeV and 12 GeV) with a proton and neutron target are considered in our paper.

## 1 Introduction

Single spin asymmetry (SSA) provides us with a powerful instrument to investigate the internal structure of the nucleon and its history can date back to the 1970s. In the early 1990s, the E704 Collaboration reported the observation of a large left-right asymmetry in  $p^\uparrow p \rightarrow \pi X$  process [1]. This demonstrated that the transverse spin effect is significant even in high energies. In order to explain the unexpected phenomenology, Sivers [2] first suggested a possible mechanism, the so-called ‘‘Sivers effect’’ today. But it was immediately criticized by Collins [3, 4], who proposed another mechanism known as the ‘‘Collins effect’’ now. Later, in Ref. [5], by considering the soft initial state interactions, it was argued that the Sivers effect might be allowed. It was not until in 2002 that people began to realize that the final state interaction plays a crucial role in leading an SSA in the SIDIS process [6]. Then after considering the gauge links, it was found that the Sivers effect, or even the Sivers distribution could exist [7], and the Sivers distribution may have different signs in the SIDIS and the Drell-Yan processes. Despite of the early theoretical debates, some phenomenological analysis [8, 9] attempted to explain the E704 data, and it was shown that the Sivers effect is important and other effects might be suppressed. But recently, an updated work [10] reported that the Collins effect is not strongly suppressed any more after a correction of a sign mistake. In all of these phenomenological works, TMD factorization were assumed, but we should be aware that the TMD factorization has not yet been proved for the  $pp \rightarrow \pi X$  process.

Contrast to the complexity of the hadron-hadron collision process, where both the initial and final states are hadrons, the semi-inclusive deep inelastic scattering (SIDIS) process provides a cleaner and simpler playground for exploring the nucleon structure. The azimuthal angle dependence of the cross section for this process has been systematically studied in Ref. [11], where different structure functions were defined according to different azimuthal angle dependences. By multiplying different orthogonal weighting functions, we can isolate different structure functions from each other, and then extract the distribution or the fragmentation functions from relevant terms. For example, the Collins or the Sivers effect has a  $\sin(\phi_h^\ell + \phi_S^\ell)$  or  $\sin(\phi_h^\ell - \phi_S^\ell)$ <sup>1</sup> modulation, respectively. Under the guidance, the HERMES [12] and COMPASS [13] Collaborations studied the  $\sin(\phi_h^\ell + \phi_S^\ell)$  and  $\sin(\phi_h^\ell - \phi_S^\ell)$  asymmetries, and have confirmed the existence of the non-zero asymmetries. In the near future, JLab also plans a high precision measurement through the SIDIS process with a beam energy upgrading to 12 GeV. More such weighting SSAs will be studied in these experiments, and we hope these new observations will bring us more knowledge about the nucleon structure.

If we turn back to the E704 observation, we find that the experiment just studied a simple un-weighted left-right asymmetry. The main reason is that in the inclusive hadron production, only one hadron is detected so that only one azimuthal angle can be defined. But in the

<sup>1</sup>  $\phi_h^\ell, \phi_S^\ell$  are also written as  $\phi_h, \phi_S$  in some other literatures, but in this paper, we will write the explicit form with a superscript  $\ell$  to address the lepton angle dependence.

SIDIS process, both the outgoing lepton and the produced hadron are measured, so we need to study a more complicated azimuthal dependence involving two azimuthal angles. However, we could still study the left-right asymmetry in the SIDIS process as the E704 experiment did. We suggest applying this method as an optional choice in analyzing the data, for it is a simple and basic quantity.

In our previous paper [15], we have studied this left-right asymmetry for the SIDIS process in the pion production. It was demonstrated that Sivers effect plays the most important role in producing a left-right asymmetry for a SIDIS process. In this paper, we will update the calculation with the new parameterizations of the DFs and FFs, and extend the calculation to the  $K^\pm$  production. As we know, the contribution from sea quarks, especially the  $s\bar{s}$  quarks, might not be ignored in the kaon production. Also, we will extend our calculation to more kinematics and targets for our prediction. HERMES kinematics with a proton target, COMPASS kinematics with a proton, deuteron, and neutron target (extracted from the  $^3\text{He}$  target), and JLab kinematics (both 6 GeV and 12 GeV) with a proton and neutron target are all considered in our paper. The main purpose of this paper is to reproduce a left-right asymmetry under the current theoretical framework, rather than to study the Sivers effect extensively. In our calculation, we will use the TMD distribution and fragmentation functions, as they may provide us a more vivid 3-dimensional picture of a nucleon. The proof of the TMD factorization for a SIDIS process can be found in Ref. [14]. We will present our calculation up to a leading order approximation.

## 2 Definition of the asymmetry and a theoretical description

Obviously, the asymmetry is a function of space coordinates, so it depends on the choice of the coordinate system. For the experiments, the most convenient choice is to choose the direction of the beam and the target polarization as the spin plane. We call it as the  $\ell p$  frame, i.e. the laboratory frame, in which we can identify left or right according to the spin plane. We might perform the measurement in a space region left to the spin plane, then in its mirror region on the right, and by their differences, we can define a left-right asymmetry which is what the E704 experiment did. We have noticed that changing the detected region from left to right is equivalence to reversing the target polarization. We can express the asymmetry as

$$A = -\frac{1}{S_T} \frac{N(\psi_S) - N(\psi_S + \pi)}{N(\psi_S) + N(\psi_S + \pi)} = -\frac{1}{S_T} \frac{d\sigma^\uparrow - d\sigma^\downarrow}{d\sigma^\uparrow + d\sigma^\downarrow}, \quad (1)$$

where  $S_T$  is the transverse polarization of the target, and  $\psi_S$  is the azimuthal angle of the spin vector. The minus sign in front of the expression is due to the fact that the detection occurred to the right of the beam, the same as that in the E704 analysis, where no weighting function is multiplied.

Before our calculation, we first give an explanation to our kinematics. For a theoretical description, the  $\ell p$  frame is not always convenient, since we usually regard the SIDIS process as a virtual Compton scattering. So it is convenient to choose the  $\gamma^*p$  frame, in which the  $z$  axis is defined along the direction of the exchanged virtual photon, and the spin plane is defined by the virtual photon and the spin vector. Thus we have two reference frames, the  $\ell p$  and the  $\gamma^*p$  frames. In the  $\ell p$  frame, we can define the transverse spin vector  $S_T$ , the azimuthal angle for the spin vector and the produced hadron as  $\psi_S$  and  $\psi_h$ , respectively. All the kinematics can be manipulated easily in this frame, but for the theoretical description, the  $\gamma^*p$  frame might be more convenient. In the  $\gamma^*p$  frame, we could define  $\phi^\ell$ ,  $\phi_S$  and  $\phi_h$  as the azimuthal angles for the lepton plane, the spin plain and the produced hadron plain, with respect to the horizontal plain in the laboratory. Then we will define  $\phi_h^\ell = \phi_h - \phi^\ell$ ,  $\phi_S^\ell = \phi_S - \phi^\ell$ , and these two angles are consistent with the Trento convention [16]<sup>2</sup>.

The explicit expression for a SIDIS process can be found in Ref. [11,17], where all the coordinate variables are defined in the  $\gamma^*p$  frame. The connection between the two frames is via a rotation by a angle  $\theta$ , due to which, a transverse spin vector in the laboratory frame has a longitudinal projection along the virtual photon [18,19]. Generally,  $\theta$  is very small and we will make further discussion later. By taking into account this, the cross section can be written as [19]:

$$\begin{aligned} & \frac{d\sigma}{dx dy d\phi_S^\ell dz d\phi_h^\ell dP_{h\perp}^2} \\ &= \frac{\alpha^2}{2sx(1-\epsilon)} \frac{\cos\theta}{1 - \sin^2\theta \sin^2\phi_S^\ell} \times \left\{ \mathcal{F}[f_1 D_1] \right. \\ & \quad - \frac{S_T \cos\theta}{\sqrt{1 - \sin^2\theta \sin^2\phi_S^\ell}} \sin(\phi_h^\ell - \phi_S^\ell) \mathcal{F} \left[ \frac{\hat{\mathbf{h}} \cdot \mathbf{p}_\perp}{M_p} f_{1T}^\perp D_1 \right] \\ & \quad - \frac{S_T \cos\theta}{\sqrt{1 - \sin^2\theta \sin^2\phi_S^\ell}} \sin(\phi_h^\ell + \phi_S^\ell) \mathcal{F} \left[ \frac{\hat{\mathbf{h}} \cdot \mathbf{k}_\perp}{M_h} h_1 H_1^\perp \right] \\ & \quad \left. + \text{other terms} \right\} \\ & \equiv d\sigma_{\text{UU}} + d\sigma_{\text{Siv}} + d\sigma_{\text{Col}} + \dots, \end{aligned} \quad (2)$$

where we use a compact notation:

$$\mathcal{F}[\omega f D] = \sum_a e_a^2 \int d^2\mathbf{p}_\perp d^2\mathbf{k}_\perp \delta^2(\mathbf{p}_\perp - \mathbf{k}_\perp - \mathbf{P}_{h\perp}/z) \omega(\mathbf{p}_\perp, \mathbf{k}_\perp) f^a(x, p_\perp^2) D^a(z, z^2 k_\perp^2), \quad (3)$$

and

$$\epsilon = \frac{1 - y - \frac{1}{4}y^2\gamma^2}{1 - y + \frac{1}{2}y^2 + \frac{1}{4}y^2\gamma^2}, \quad \hat{\mathbf{h}} \equiv \mathbf{P}_{h\perp}/|\mathbf{P}_{h\perp}|. \quad (4)$$

<sup>2</sup> These two azimuthal angles are denoted as  $\phi_h$  and  $\phi_S$  in the Ref. [16], but the notations are for other uses in our paper.

**Table 1.** An estimation on  $\sin \theta$ 

	HERMES	JLab	
		6 GeV	12 GeV
$\langle x \rangle$	0.09	0.23	0.23
$\langle y \rangle$	0.54	0.6	0.57
$\langle Q^2 \rangle$	2.41 GeV <sup>2</sup>	1.8 GeV <sup>2</sup>	2.5 GeV <sup>2</sup>
$\langle \sin \theta \rangle$	0.073	0.19	0.17

First, we make a first approximation that  $\theta$  is small (We will give a detailed discussion later), thus the  $\ell p$  and  $\gamma^* p$  frames are of no difference. Now under this approximation, we can use the kinematics defined in the  $\gamma^* p$  frame instead to analyze the asymmetry defined in Eq. 1,

$$A_{UT}(x, y, z, P_{h\perp}) \approx -\frac{1}{S_T} \frac{\int d\phi_S^\ell d\phi_h^\ell (d\sigma_{\text{Siv}} + d\sigma_{\text{Coll}} + \dots)}{\int d\phi_S^\ell d\phi_h^\ell d\sigma_{\text{UU}}} \quad (5)$$

Next, we change the integral measure from  $d\phi_S^\ell d\phi_h^\ell$  to  $d\phi^\ell d\phi_h$  (The jacobian  $|J| = 1$ ), and perform the integral over  $\phi^\ell$ . We notice that  $\sin \phi_S^\ell$  explicitly depends on  $\phi^\ell$  and all the convolution integrals  $\mathcal{F}$  are independent of  $\phi^\ell$ . For the azimuthal angle dependence, we find that all the factors are oscillation functions of  $\phi^\ell$  except  $\sin(\phi_h - \phi_S)$ , which is  $\phi^\ell$ -independent. So after integrating over  $\phi^\ell$ , we find that Siverts effect is  $o(1)$ , but other terms such as the Collins effect are  $o(\sin^2 \theta)$  (See detailed discussion in Ref. [15]). So Siverts effect is dominant and other effects are suppressed in our analysis. We could also understand this result as the following. If we ignore the angle  $\theta$ , we could set the  $\gamma^* p$  frame equal to the  $\ell p$  frame in the laboratory. In the E704 method, only one azimuthal angle was involved in fact, i.e.  $\phi_h$  in our notation (not  $\phi_h^\ell$ ), and the lepton angle  $\phi^\ell$  in not included in the analysis. For a SIDIS process, only the Siverts effect is independent of the lepton plane, so it is not strange that the Siverts effect plays the most important role in leading an left-right asymmetry.

We could make an estimation on the effect resulted from the angle  $\theta$ . This angle can be calculated from the kinematical variables [19]

$$\sin \theta = \gamma \sqrt{\frac{1 - y - \frac{1}{4}y^2\gamma^2}{1 + \gamma^2}}, \quad \gamma = 2xM_p/Q. \quad (6)$$

We replace each variable by its average value to estimate the mean value of  $\sin \theta$  for the HERMES and JLab experiments.

The estimated result is shown in Table 1, and we find that for most instance, the direction of the virtual photon is very close to the direction of the incident beam. Therefore, for convenience, the Collins effect which is not known so clearly yet is not considered in our analysis.

### 3 Parametrization for distribution and fragmentation functions

As a preparation for our calculation, we will present the parametrization for the distribution and fragmentation functions we will use in this section.

For the Siverts functions, there are already some model calculations [20], but we would use a phenomenological parameterization for the Siverts functions. We should be cautious that a universal transverse momentum dependent Siverts distribution for different processes does not exist [21]. Fortunately, we will calculate for the SIDIS process, and the parametrization of the Siverts function is also from the SIDIS data. The Siverts effect has already been studied by HERMES and COMPASS Collaborations, and extractions on the Siverts functions for the  $u$  and  $d$  quarks were already obtained [8, 22, 23, 24]. But all these results were under low statistics and assumed the existence of a symmetric and negligibly small Siverts sea. Recently, the HERMES Collaboration has provided much higher statistic data on the  $A_{UT}^{\sin(\phi_h - \phi_S)}$  azimuthal asymmetry [25]. Besides the charged pion production, neutral pion and charged kaon azimuthal asymmetries were also analyzed. Also, the COMPASS Collaboration separated the charged pion and charged kaon asymmetries from the charged hadron production measurement [?, 26]. These SIDIS experimental data on the Siverts asymmetries for the pion and kaon production give us an opportunity to study the sea-quark Siverts functions for the  $\bar{u}$ ,  $\bar{d}$ ,  $s$ , and  $\bar{s}$  quarks. With these data, in Ref. [27], the extraction of these functions was improved and the first estimates of the sea-quark Siverts functions were presented. The Siverts function is parameterized in the form

$$f_{1T}^{\perp q}(x, p_\perp^2) = -\frac{M_p}{p_\perp} \mathcal{N}_q(x) f_q(x) g(p_\perp^2) h(p_\perp^2), \quad (7)$$

$$\mathcal{N}_q(x) = N_q x_q^\alpha (1-x)_q^\beta \frac{(\alpha_q + \beta_q)^{(\alpha_q + \beta_q)}}{\alpha_q^{\alpha_q} \beta_q^{\beta_q}}, \quad (8)$$

$$g(p_\perp^2) = \frac{e^{-p_\perp^2/\langle p_\perp^2 \rangle}}{\pi \langle p_\perp^2 \rangle}, \quad h(p_\perp^2) = \sqrt{2} e \frac{p_\perp}{M'} e^{-p_\perp^2/\langle M'^2 \rangle}. \quad (9)$$

All the parameters can be found in Ref. [27]. In the above parametrization,  $f(x)$  is the unpolarized parton distribution functions, and we adopt the CTEQ6L parametrization [28] as an input. We plot the Siverts functions for different quark flavors in Fig. 1

For the fragmentation functions, all the former analysis of the fragmentation functions were based exclusively on the single-inclusive  $e^+e^-$  annihilation (SIA) data and have been chosen the most simple functional form  $N_i z^{\alpha_i} (1-z)^{\beta_i}$  to parametrize the  $D_i^H$ . But in these experiments, information on the quark and anti-quark fragmentation is always combined, for it always refers to the charge sum for certain hadron species, e.g.  $\pi^+ + \pi^-$ . In order to distinguish ‘‘valence’’ from ‘‘sea’’ fragmentation, some assumptions were proposed, e.g., in Ref. [29],  $D_u^{\pi^+}/D_u^{\pi^+} = (1-z)$  was assumed. In the last few years several one-particle inclusive measurements coming from both the proton-proton

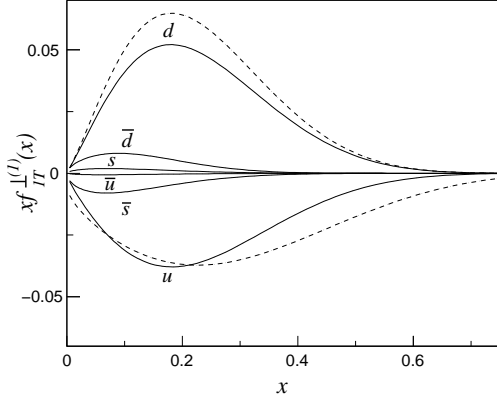


**Fig. 1.** Sivers functions for different quark flavors. Solid curves are the new results according to Ref. [27], and dashed curves are that according to Ref. [22]

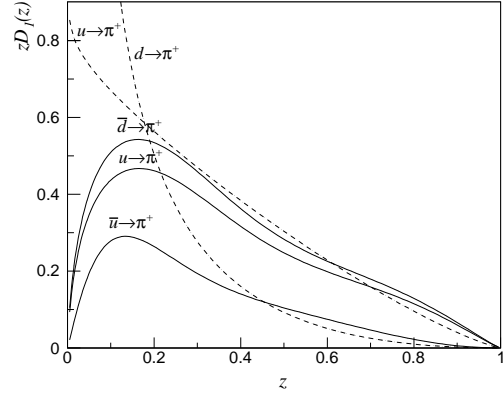


**Fig. 2.** Fragmentation functions for  $\pi^+$ . Solid curves are the results according to Ref. [30], and dashed curves are the results used in Ref. [15].

collisions and the deep-inelastic lepton-nucleon scattering gave an opportunity to weigh each quark contribution in the hadronization process. In Ref. [30], a global analysis was taken for the first time to analyze the individual fragmentation functions for all flavors as well as gluons. A more flexible input is used

$$D_i^H(z, \mu_0) = \frac{N_i z^{\alpha_i} (1-z)^{\beta_i} [1 + \gamma_i (1-z)^{\delta_i}]}{B[2 + \alpha_i, \beta_i + 1] + \gamma_i B[2 + \alpha_i, \beta_i + \delta_i + 1]}, \quad (10)$$

where  $B[a, b]$  is the Beta-function and  $N_i$  is normalized to represent the contribution of  $D_i^H$  to the sum rule. For the fragmentation to  $\pi^+$ , the isospin symmetry for the sea fragmentation functions is imposed, i.e.,

$$D_{\bar{u}}^{\pi^+} = D_d^{\pi^+}. \quad (11)$$

But slightly different normalization in the  $q + \bar{q}$  sum is allowed:

$$D_{d+\bar{d}}^{\pi^+} = N D_{u+\bar{u}}^{\pi^+}. \quad (12)$$

For the strange quarks it is assumed that

$$D_s^{\pi^+} = D_{\bar{s}}^{\pi^+} = N' D_{\bar{u}}^{\pi^+}. \quad (13)$$

For the charged kaons, it is assumed that the unfavored fragmentation functions are the same,

$$D_{\bar{u}}^{K^+} = D_s^{K^+} = D_d^{K^+} = D_{\bar{d}}^{K^+}. \quad (14)$$

From these relations, the unfavored fragmentation functions can be distinguished from the favored ones. Detailed parametrization for the integrated fragmentation function  $D(z)$  can be found in Ref. [30]. We present the numerical results for the charged pion and kaon fragmentation functions in Fig. 2 and Fig. 3. We notice that in this parametrization, the  $\bar{s} \rightarrow K^+$  process is the most favored one, which means that sea quarks, especially  $\bar{s}$  quark, might contribute significantly, although sea quark distributions are small compared with the valence quarks. So

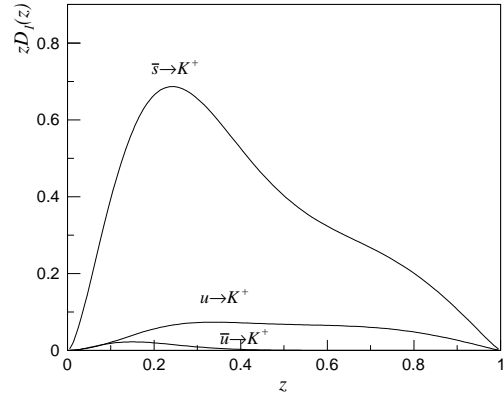


**Fig. 3.** Fragmentation functions for  $K^+$  according to Ref. [30]

measurements on the kaon production may help us to know more about the  $s(\bar{s})$  distribution. In our calculation, we need the TMD fragmentation function, and we adopt a Gaussian assumption

$$D_1(z, z^2 k_{\perp}^2) = D_1(z) \frac{\exp(-z^2 k_{\perp}^2 / R^2)}{\pi R^2}, \quad (15)$$

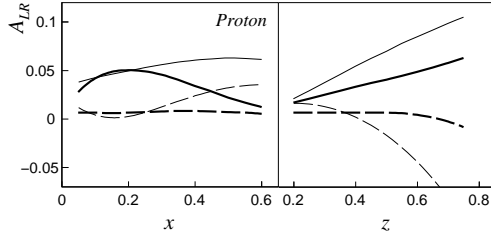
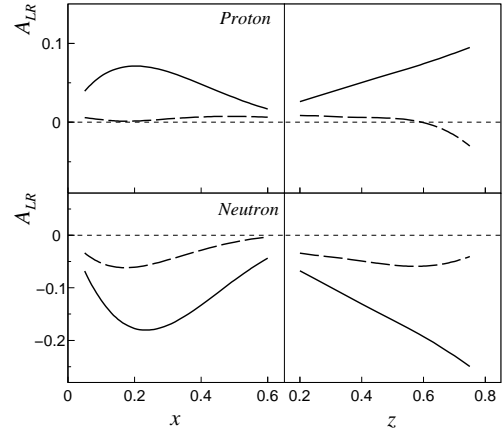
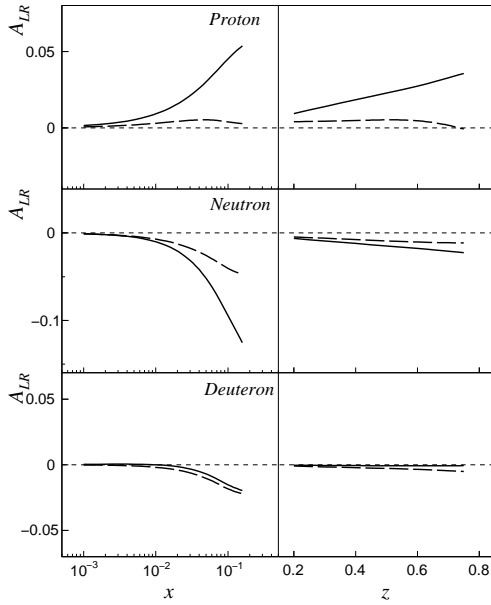
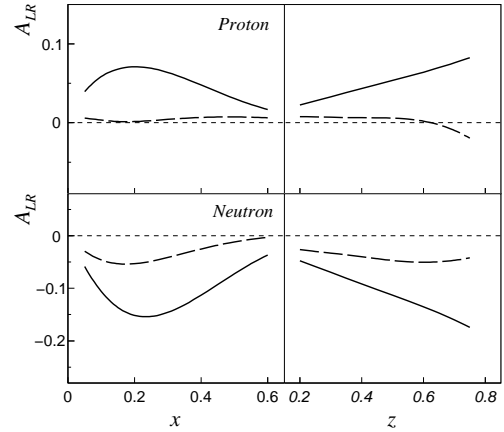
with  $R^2 = 0.2 \text{ GeV}^2$  suggested in Ref. [31].

## 4 Numerical calculations

The kinematical cuts used in the calculation are shown in Table 2. For the HERMES experiment, only the proton target is calculated. For the COMPASS experiment, the proton, neutron and deuteron targets are all considered, while for the JLab experiment, the proton and neutron targets are assumed. In fact there is no free neutron target, and in experiments the polarized  $^3\text{He}$  is used. The effective asymmetry on a free neutron can be extracted from a  $^3\text{He}$  target asymmetry. Detailed discussions can be found in some theoretical works [32] and a JLab's pro-

**Table 2.** Kinematics

	HERMES	COMPASS	JLab1		JLab2	
			proton	neutron	proton	neutron
$p_{\text{beam}}/\text{GeV}$	27.6	160	6	6	12	12
$Q^2/\text{GeV}^2$	> 1	> 1	> 1	1.3 ~ 3.1	> 1	> 1
$W^2/\text{GeV}^2$	> 10	> 25	> 4	5.4 ~ 9.3	> 4	> 2.3
$x$	0.023 ~ 0.4		0.1 ~ 0.6	0.13 ~ 0.4	0.05 ~ 0.7	0.05 ~ 0.55
$y$	0.1 ~ 0.85	0.1 ~ 0.9	0.4 ~ 0.85	0.68 ~ 0.86	0.2 ~ 0.85	0.34 ~ 0.9
$z$	0.2 ~ 0.7	0.2 ~ 1	0.4 ~ 0.7	0.46 ~ 0.59	0.4 ~ 0.7	0.3 ~ 0.7

**Fig. 4.** The  $x$  and  $z$ -dependence of the left-right asymmetry for  $\pi^\pm$  production on HERMES kinematics. Solid lines for  $\pi^+$  and dashed lines for  $\pi^-$ . Thick curves are our results and thin curves are results from Ref. [15]**Fig. 6.** Similar as Fig. 4, but at JLab kinematics with a beam energy of 6 GeV.**Fig. 5.** Similar as Fig. 4, but at COMPASS kinematics.**Fig. 7.** Similar as Fig. 4, but at JLab kinematics with a beam energy of 12 GeV.

posal [33]. We will investigate the  $x$  and  $z$  dependence<sup>3</sup> of the asymmetries.

First, we present our results on  $\pi^\pm$  production at different kinematics. Fig. 4 - Fig. 7 show the results of the

<sup>3</sup> The E704 experiment only showed the dependence on  $x_F$ , i.e. approximate  $z$  here.

left-right asymmetry. In Fig. 4, we make a comparison with the results already obtained in Ref. [15], and we find that the two results are a little different. For the  $x$ -dependence of the asymmetry, our new results are suppressed when  $x$  increases. We can find the reason from the parametrization for Sivvers functions as Fig. 1 shows. The new parametrization shows that at large  $x$  region

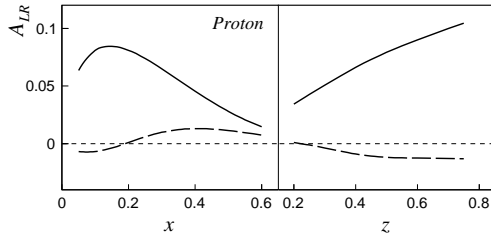


**Fig. 8.** The  $x$  and  $z$ -dependence of the left-right asymmetry for  $K^\pm$  production on HERMES kinematics. Solid lines for  $K^+$  and dashed lines for  $K^-$ .

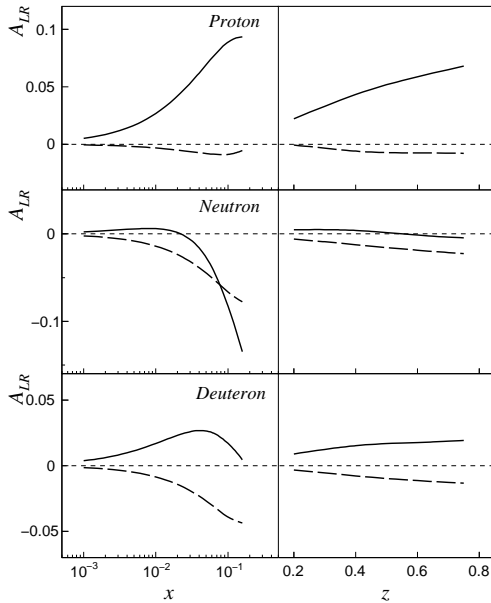


**Fig. 9.** Similar as Fig. 8, but at COMPASS kinematics.

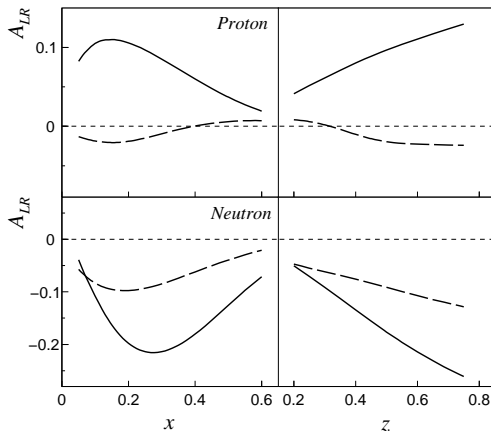


**Fig. 10.** Similar as Fig. 8, but at JLab kinematics with a beam energy of 6 GeV.

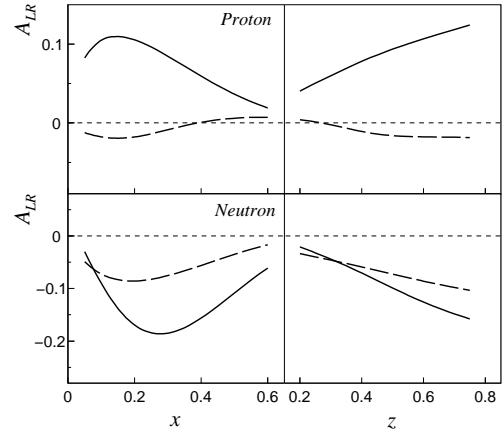


**Fig. 11.** Similar as Fig. 8, but at JLab kinematics with a beam energy of 12 GeV.

( $x > 0.3$ ), the  $u$  quark distribution falls down much faster than a previous parametrization, while the  $d$  quark distribution does not change so much. Notice that the  $u$  quark distribution gives a positive contribution, then we could understand our new results. For the  $z$ -dependence, the difference results not only from the distributions, but also from different parametrizations of the fragmentation functions. So we can say that our results are sensitive to the parametrization.

Next we will extend our calculation to the  $K^\pm$  production, and the results are shown in Fig. 8 - Fig. 11. The  $K^+$  production is quite similar to that of  $\pi^+$ , but for the  $K^-$  production, we should be cautious.  $K^-$  is made up of a  $\bar{u}$  and an  $s$  quark. So the sea quark contribution (from  $\bar{u}$  and  $s$ ) might be enhanced due to the favored fragmentation process, while the valence quark contribution would be suppressed. Thus, the  $K^-$  production is a good way to study the sea quark distributions and the unfavored fragmentation processes. Notice that the Siverts distributions of the  $\bar{u}$  and  $s$  quarks given in Ref. [27] are so small with a large uncertainty that even their signs are not determined within the error, so our prediction must cover a large uncertainty area. Nevertheless, we hope that our results will be helpful to the future experiments and we expect that further experiments with a high precision will clarify the detail.

## 5 Conclusion

Following the E704 analysis, we reanalyzed the left-right asymmetry in the SIDIS process with the new Siverts functions and fragmentation functions. In this paper, we considered all the flavor contributions, including the sea quarks. We extended our analysis to the  $K^\pm$  production process, and meanwhile to various kinematics with different targets. We found that our results are sensitive to the parametrization form of the distribution and fragmentation functions, so we consider it necessary to perform higher precision measurements to constrain the parametrization.

Our prescription originated from the E704 experiment is an optional and simple way analyzing the data. In this prescription, no weighting functions are multiplied, although it might not give any more information. We suggest that relevant experiment collaborations could present their data in this new way as an optional choice for further theoretical studies.

## Acknowledgement

This work is partially supported by National Natural Science Foundation of China (No. 10375002, No. 10675004, No. 10721063 and No. 10975003), by the Key Grant Project of Chinese Ministry of Education (No. 305001), by the Research Fund for the Doctoral Program of Higher Education (China).

## References

1. D. L. Adams, *et al.*, (FNAL E704 Collaboration), Phys. Lett. B **261**, 201 (1991); Phys. Lett. B **264**, 462 (1991).
2. D. W. Sivers, Phys. Rev. D **41**, 83 (1990); D. W. Sivers, Phys. Rev. D **43**, 261 (1991).
3. J. C. Collins, Nucl. Phys. B **396**, 161 (1993).
4. J. C. Collins, S. F. Heppelmann, and G. A. Ladinsky, Nucl. Phys. B **420**, 565 (1994).
5. M. Anselmino, M. Boglione, and F. Murgia, Phys. Lett. B **362**, 164 (1995).
6. S. J. Brodsky, D. S. Hwang, and I. Schmidt, Phys. Lett. B **530**, 99 (2002); S. J. Brodsky, P. Hoyer, N. Marchals, S. Peigne, and F. Sannino, Phys. Rev. D **65**, 114025 (2002).
7. J. C. Collins, Phys. Lett. B **536**, 43 (2002); X. Ji and F. Yuan, Phys. Lett. B **543**, 66 (2002); A.V. Belitsky, X. Ji, and F. Yuan, Nucl. Phys. B **656**, 165 (2003).
8. M. Anselmino, M. Boglione, U. D'Alesio, E. Leader, F. Murgia, Phys. Rev. D **71**, 014002 (2005).
9. M. Anselmino, M. Boglione, U. D'Alesio, E. Leader, S. Melis, and F. Murgia, Phys. Rev. D **73**, 014020 (2006).
10. M. Anselmino, M. Boglione, U. D'Alesio, E. Leader, S. Melis, and F. Murgia, arXiv:0809.3743.
11. A. Kotzinian, Nucl. Phys. B **441**, 234 (1995).
12. A. Airapetian, *et al.*, (HERMES Collaboration), Phys. Rev. Lett. **84** 4047 (2000); Phys. Rev. D **64** 097101 (2001); Phys. Lett. B **562**, 182 (2003); Phys. Rev. Lett. **94**, 012002 (2005).
13. V.Y. Alexakhin, *et al.*, [COMPASS Collaboration], Phys. Rev. Lett. **94**, 202002 (2005); E.S. Ageev, *et al.*, [COMPASS Collaboration], Nucl. Phys. B **765**, 31 (2007); Anna Martin (On behalf of the COMPASS Collaboration), Czech. J. Phys. **56**, F33 (2006), hep-ex/0702002.
14. X. Ji, J.-P. Ma, F. Yuan, Phys. Lett. B **597**, 299 (2004); X. Ji, J.-P. Ma, F. Yuan, Phys. Rev. D **71**, 034005 (2005).
15. J. She, Y. Mao, B.-Q. Ma, Phys. Lett. B **666**, 355 (2008).
16. A. Bacchetta, U. D'Alesio, M. Diehl and C. A. Miller, Phys. Rev. D **70**, 117504 (2004).
17. A. Bacchetta, M. Diehl, K. Goeke, A. Metz, P.J. Mulders, and M. Schlegel, JHEP 0702: 093 (2007).
18. K. A. Oganessyan, P. J. Mulders, E. De Sanctis, L. S. Asilyan, Nucl. Phys. A **711**, 89 (2002); K. A. Oganessyan, P. J. Mulders, E. De Sanctis, Phys. Lett. B **532**, 87 (2002).
19. M. Diehl and S. Sapeta, Eur. Phys. J. C **41**, 515 (2005).
20. L. P. Gamberg, G. R. Goldstein, and K. A. Oganessyan, Phys. Rev. D **67**, 071504(R) (2003); A. Bacchetta, A. Schaefer, and J. J. Yang, Phys. Lett. B **578**, 109 (2004); A. Bacchetta, F. Conti, and M. Radici, Phys. Rev. D **78**, 074010 (2008); F. Yuan, Phys. Lett. B **575**, 45 (2003); I. O. Cherednikov, U. D'Alesio, N.I. Kochelev, and F. Murgia, Phys. Lett. B **642**, 39 (2006); A. Courtoy, F. Fratini, S. Scopetta, and V. Vento, Phys. Rev. D **78**, 034002 (2008); A. Courtoy, S. Scopetta, and V. Vento, Phys. Rev. D **79**, 074001 (2009).
21. C.J. Bomhof, P.J. Mulders, Nucl. Phys. B **795**, 409 (2008).
22. M. Anselmino *et al.*, Phys. Rev. D **72**, 094007 (2005), Erratum-ibid. D **72** 099903, (2005).
23. A. V. Efremov, K. Goeke, S. Menzel, A. Metz, and P. Schweitzer, Phys. Lett. B **612**, 233 (2005).
24. J. C. Collins, A. V. Efremov, K. Goeke, S. Menzel, A. Metz, and P. Schweitzer, Phys. Rev. D **73**, 014021 (2006).
25. M. Diefenthaler (HERMES), arXiv: 0706.2242; A. Airapetian *et al.* (HERMES), Phys. Rev. Lett. **103**, 152002, 2009.
26. M. Alekseev *et al.* (COMPASS), Phys. Lett. B **673**, 127 (2009).
27. M. Anselmino *et al.*, Eur. Phys. J. A **39**, 89 (2009).
28. J. Pumplin, D. R. Stump, J. Huston, H. L. Lai, P. Nadolsky, and W.K. Tung, JHEP **0207**, 012 (2002).
29. S. Kretzer, Phys. Rev. D **62**, 054001 (2000).
30. D. de Florian, R. Sassot, and M. Stratmann, Phys. Rev. D **75**, 114010 (2007).
31. M. Anselmino, M. Boglione, U. D'Alesio, A. Kotzinian, F. Murgia, A. Prokudin, Phys. Rev. D **71**, 074006 (2005).
32. S. J. Brodsky and S. Gardner, Phys. Lett. B **643**, 22 (2006); S. Scopetta, Phys. Rev. D **75**, 054005 (2007).
33. J.-P. Chen and J.-C. Peng, JLab-PAC29.